Journal of Energy, Environmental & Chemical Engineering
2017; 2(2): 25-31
http://www.sciencepublishinggroup.com/j/jeece
doi: 10.11648/j.jeece.20170202.12

NO_X Emission Reduction by Non Thermal Plasma Technique

Nasser Morgan[1, 3, *], Diaa Ibrahim[2], Ahmed Samir[3]

[1]Physics Department, Faculty of Science, Al Azhar University, Cairo, Egypt
[2]Egyptian Academy for Engineering and Advanced Technology, Cairo, Egypt
[3]Center of Plasma Technology, Al Azhar University, Cairo, Egypt

Email address:

Nassernm_2000@yahoo.com (N. Morgan), die2070@yahoo.com (D. Ibrahim), ahmed_samir_aly@yahoo.com (A. Samir)
[*]Corresponding author

To cite this article:

Nasser Morgan, Diaa Ibrahim, Ahmed Samir. NO_X Emission Reduction by Non Thermal Plasma Technique. *Journal of Energy, Environmental & Chemical Engineering*. Vol. 2, No. 2, 2017, pp. 25-31. doi: 10.11648/j.jeece.20170202.12

Received: June 9, 2017; **Accepted**: July 4, 2017; **Published**: July 24, 2017

Abstract: The current work demonstrates the feasibility of atmospheric pressure non-thermal plasma technique for NO_x pollution control. Atmospheric pressure dielectric barrier discharge plasma reactor has been constructed for the treatment of the exhaust of 4kWs free load diesel engine. The nature and properties of the discharge were identified through studying electrical characterization of the discharge cell. The effect of applied voltage, discharge power and discharge length on the removal and energy efficiency of NO_x has been investigated. Different parameters including, NO_x removal efficiency, specific energy density and energy cost per molecule have been calculated, analyzed and interpreted. It has been found that the removal efficiency of NO_x was varied from (16%-74%) at energy cost of values varied from (123-390 eV/molecule). The obtained data represents promising results and offers a solution for NO_x pollution reduction.

Keywords: Non Thermal Plasma, Apdbd, NO_x Reduction, Efficiency, Energy Cost, Energy Density

1. Introduction

NOx gases are one of the most harmful pollutants to human health and environment which can lead to cancer, respiratory and cardiovascular diseases [1]. Air pollution is in general associated with health impacts on fertility, pregnancy, newborn and children according to world health organization WHO [2]. In 2016 European Environment Agency (EEA) reported that NO_x pollution is responsible for tens of thousands of early deaths across Europe each year [3]. There are some indirect ways by which NO_x can affect human health, as example, acid rains accelerates corrosion of buildings and cause acidification of lakes and streams [4]. NO_X sources are generally originated from fossil fuels burning in thermal power stations, motor vehicles, steel production factories and chemical plants. Automobiles and other mobile sources contribute to 50% of the NOx emission [5]. Engines produce exhaust fumes particularly rich in oxygen; as a result the conventional catalytic converters are not suitable for converting the generated NO_x into nitrogen [6]. Recently, some researchers have used an aqueous urea solution to convert the NO_x into harmless nitrogen via various chemical reactions in a special selective reduction catalyst (SCR) [7]. The aqueous urea solution was carried in a separate tank inside the car and needs to be topped up every now and again, usually while the vehicle is being serviced [7]. Using ammonia has some disadvantage, a low dosage of urea does not yield efficient NO_x reduction, and a high dosage results in undesirable ammonia emissions. At temperatures below 200°C, aqueous urea solution tends to form residues that eventually clog up the SCR catalyst [7]. In recent years, nonthermal plasmas have been widely employed as one of the promising technologies for pollution control with high removal efficiencies and low energy cost [8-13]. Plasma is a chemically reactive medium inside which large concentrations of active species are generated. Ions, excited molecules and atoms, photons, energetic electrons and active species represent the main components of plasma [13]. Nonthermal plasmas (NTP) possess a lower translational temperature (< 300K) of ions and neutral atoms, while possessing electrons of high energy (> 1 eV or 11,000 K) [13, 14]. Energetic electrons in NTP can easily break most

chemical bonds, make NTP suitable for environmental applications. Dielectric barrier discharge (DBD) is one of the most applicable plasma techniques that work at atmospheric pressure [13-16]. DBD is inhomogeneous filamentary discharge plasma that works at atmospheric pressure, requires alternating voltages for its operation. The main advantage of DBD is that it works under atmospheric pressure, consumes low power and ease of operation. A massive number of researchers had applied DBD for NO_x reduction [17-19]. Some used packed bed DBD reactors [20, 21] and others used catalytic assisted DBD reactor [22, 23].

The object of the present work is to investigate an efficient catalytic free, dielectric barrier discharge reactor constructed for NO_x reduction. The source of NO_x gas was taken from the exhaust of a 4kW diesel generator operated on no load. Most of the exhaust is let off to atmosphere with only a small part of the exhaust was directed to the discharge cell and withdrawn by the pump of gas analyzer at flow rate of about 5 L/min. Different parameters including, applied voltage, discharge power, and discharge length have been investigated experimentally to achieve the maximum NO_x reduction percentage. Different parameters including, NO_x removal efficiency, specific energy density and energy cost per molecule have been calculated and discussed.

2. Experimental Setup

Schematic diagram of the co-axial DBD system is shown in figure1.

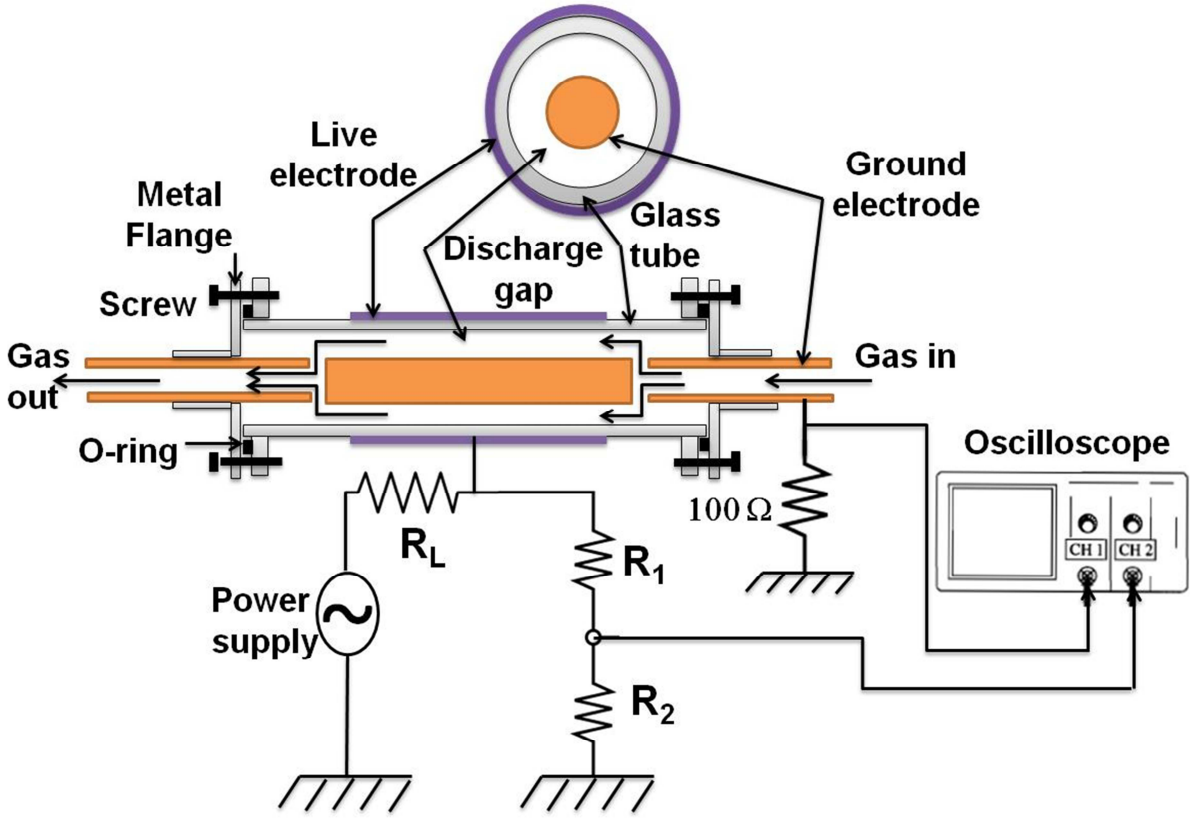

Figure 1. *Schematic diagram for coaxial DBD.*

The discharge cell consists of two coaxial electrodes separated by a Pyrex glass tube with a length of 140 cm, inner and outer diameter of 1.2 and 1.5 cm respectively. The ground electrode was made of copper rod with a diameter of 0.8 cm and 120 cm in length. The ground electrode was drilled at one of its ends and connected to the exhaust of the a 4 kW diesel engine operated at no load to let the treated gas enter the discharge zone. A paste graphite layer was painted on the outer surface of the Pyrex tube then connected to the live terminal of the power supply representing the live electrode. The graphite layer length could be varied from 10 cm to 120 cm to change the discharge zone volume. The gap space between the electrodes was kept constant at 2 mm. Step up high voltage transformer (12 kV, 15 mA, 50 Hz) was used as a sinusoidal high voltage source and connected to the life electrode through a protecting limiting resistance R_L. The current and voltage waveforms were recorded experimentally by 100 MHz two channels, digital storage oscilloscope (Type HM1508). Channel one was connected to a potential divider (R_1:R_2) to measure the applied voltage on the discharge cell, the other channel was connected to a 100 ohm resistance inserted between the inner electrode and the ground to measure the discharge current. The discharge power was calculated using the Q-V Lissajous figure following the method of Manley [24, 25]. The accumulated charge was measured by replacing the 100 ohm resistance by 10 nF capacitor. The treated gas was directed to multi gas analyzer (model Teknotest 488) at flow rate 5 L/min to measure NO_x

concentration. The initial concentration of the NO_x was kept constant at 200 ppt.

3. Results and Discussion

3.1. Electrical Characterization

3.1.1. Current- Voltage Waveform

The current - voltage oscillogram of the coaxial DBD reactor operated at atmospheric pressure and ambient temperature is shown in figure 2. The figure shows that as the gap voltage increases, a displacement current starts to flow through the reactor. When the gap voltage reaches the electrical breakdown value, a number sharp filaments appear over the current signal represent the micro-discharges mode of the DBD.

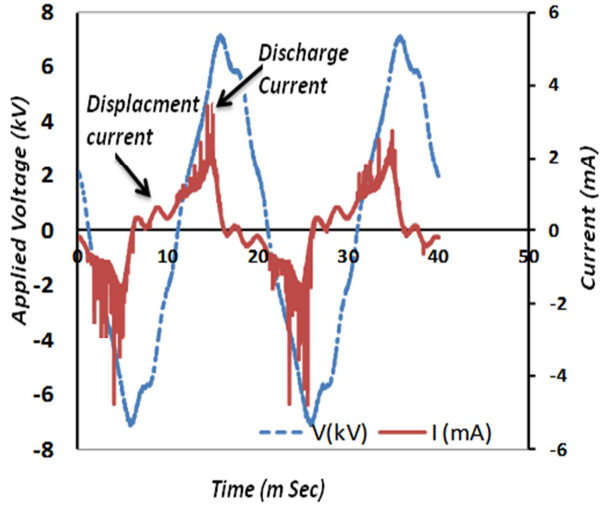

Figure 2. *Current-Voltage oscillogram.*

To understand the current-voltage waveform of DBD an electric model of the discharge, schematically described in figure 3 cell will used [26].

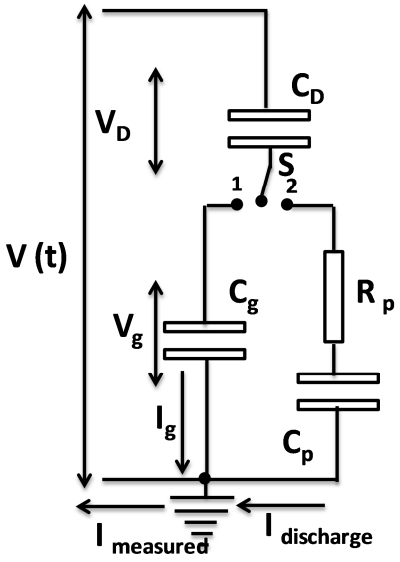

Figure 3. *DBD circuit model.*

C_D and C_g represent the capacitance of dielectric material adjacent to one of two electrodes and the gap capacitance respectively. C_p and R_p represent the capacitance and resistance that modeling the electric response of plasma. When the applied voltage across the gap is less than the discharge voltage, switch S in position 1 in figure 3, there is no electrical breakdown and the applied voltage is divided between the discharge gap and dielectric material and a displacement current $I_{displacement}$ (t) will flow in the circuit, given by formula (1):

$$I_{displacment}(t) = \frac{C_D C_g}{C_D + C_g} \frac{dV}{dt} \quad (1)$$

When the applied voltage reaches the breakdown voltage, switch S is in position 2, the discharge current goes on with numerous tiny breakdown channels referred as micro discharges superimposed on the current waveform as shown in figure 2. A filamentary discharge is initiated when a high voltage is applied to the electrodes such that the electric field in the open gap equals or exceeds the breakdown strength of the ambient gas. The mechanism of creation of the filaments could be explained as follow: as the applied voltage increases the background free electrons are accelerated in the electric field to energies equal or exceed the ionization energy of the gas, and create an avalanche in which the number of electrons doubles with each generation of ionizing collisions. The high mobility of the electrons compared to the ions allows the electron swarm to move across the gap at a time measured in nanoseconds that appear in the current waveform as a pulse with 100 nanosecond duration. The electrons leave behind the slower ions, and various excited and active species that may undergo further chemical reactions [27]. The microdischarge filaments schematically represented in figure 4 can be characterized as weakly ionized plasmas with properties resembling those of transient high pressure glow discharges [28].

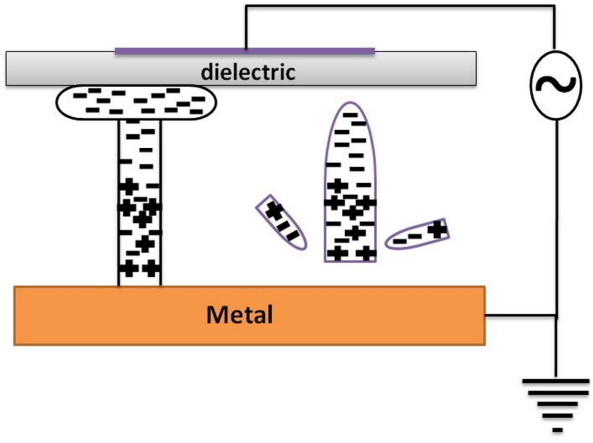

Figure 4. *Schematic diagram of micro discharge formation.*

The number of microdischarge channels was proportional to the applied voltage between the two electrodes. The discharge current cycles are a little bit different from each other in the microdischarge density and peak intensity, this

because one of the two electrodes is covered with a dielectric material while the other is naked. When the electron swarm reaches the opposite electrode, the electrons spread out over the insulating surface, counteracting the positive charge on the instantaneous anode. This factor, combined with the cloud of slower ions left behind, reduces the electric field in the vicinity of the filament and terminates any further ionization along the original track in time scales of tens of nanoseconds.

3.1.2. Consumed Power Determination

The consumed power was calculated following the original the work of Manley, who had used charge-voltage Lissajous figures to determine the average consumed power during the discharge [24]. Figure 5 shows the charge-voltage characteristic plot (Q-V plot), which appears as a parallelogram where Q_{max} is the maximum charge transferred through the gas gap. The appearance of two distinct slopes of the Q-V plot indicates the two values of effective discharge capacitance, dielectric discharge capacitance C_D and gas capacitance C_g as previously described in the equivalent circuit of DBD.

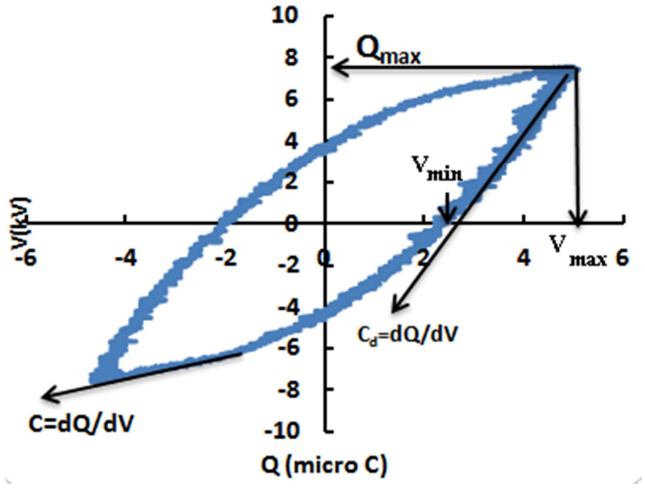

Figure 5. *Charge-Voltage Lissajous figure at discharge length 120 cm and applied voltage 5 kV.*

The DBD power formula described in equation (2) relates the total power P to the operating frequency f, the peak voltage V_{max} and the minimum discharge voltage V_{min} at which microdischarges are observed in the discharge gap with the capacitances of the dielectric (C_D) and the discharge gap (C_g).

$$\left\{\begin{array}{c} p = \frac{1}{T}\int_0^T v(t)i(t)dt; i(t) = \frac{dQ}{dt} \\ \therefore\ p = \frac{1}{T}\int_0^T v(t)dQ \\ p = 4fC_D^2(C_D + C_g)^{-1}V_{min}(V_{max} - V_{min}) \end{array}\right\} \quad (2)$$

Figure 6 shows the variation of consumed power inside the discharge cell as a function of the applied voltage at different discharge length. The figure shows a linear relation between the consumed power and both the applied voltage at each discharge length. The consumed power also increases with increasing the discharge length attributed to the increase in discharge volume that needs more energy to sustain the plasma.

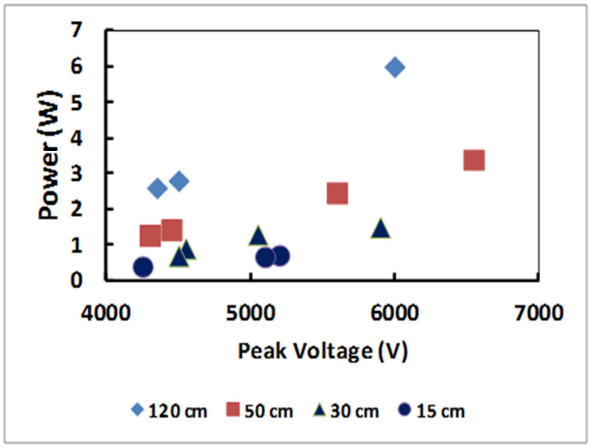

Figure 6. *Discharge power as a function applied voltage at different discharge length and constant flow rate.*

Figure 7 shows the relation between consumed power and the maximum amount of charges deposited inside the discharge cell in each cycle at different discharge length. It is seen from the figure that the amount of charge deposit per cycle is a power dependent, as the power increases the amount of deposit charge increases. The amount of deposit charge is also a function of the discharge length, as the discharge length increases the discharge volume also increases followed by an increase in depositing charge inside the discharge gap.

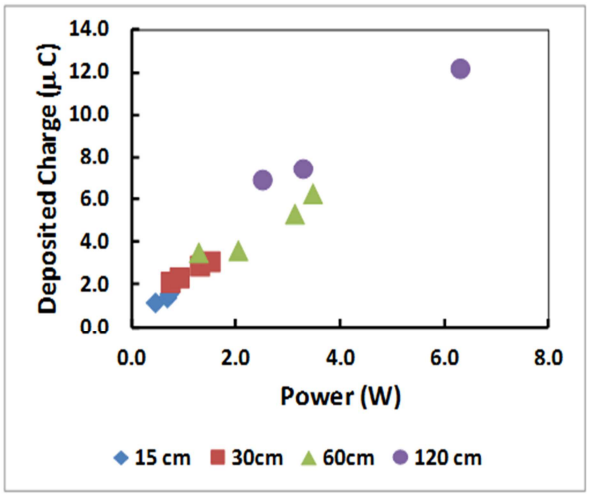

Figure 7. *Charge deposited as a function of the consumed power.*

3.2. NO_x Removal Efficiency

The NO_x gas with a mixture of hydrocarbons and air was taken from the exhaust of a 4kW diesel generator operated at no load. The exhaust was first collected in a gas container, then directed to the discharge cell through the pump of the gas analyzer at constant flow rate of 5 L/min. The NO_x removal efficiency was described as follow:

$$\eta_{NOx}\% = \frac{NO_{x_{initial}} - NO_{x_{final}}}{NOx_{initial}} \times 100 \quad (3)$$

$$NO_{x_{initial}}: initial\ concentration\ of\ NO_x\ in\ ppm$$

$$NO_{x_{final}}: final\ concentration\ of\ NO_x\ in\ ppm$$

The dependence of NO_x removal efficiency on the applied voltage and discharge length can bee seen in figure 8. It has been found that the NO_x removal efficiency is an increasing function of the applied voltage which might be attributed to the increase of both the electron density and the electron temperature inside the discharge channels of DBD.

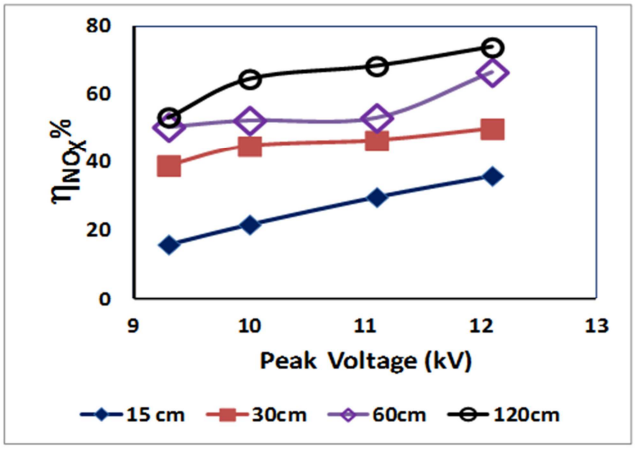

Figure 8. *NO_x removal efficiency as a function of applied voltage at different discharge length.*

The electrons impact collisions inside the discharge zone cause a lot of dissociative reactions of oxygen, nitrogen and water vapor molecules those produce free radicals, like $O^{\bullet}$, $OH^{\bullet}$, N and O_3 interact with NO and NO_2 to finally produce N_2 and nitric acid as described in table 1. The reactions pathway is divided into two main categories, oxidative and reductive reactions [29]. Oxidation is the dominant process, particularly when the O_2 concentration is 5% or higher [30]. The oxidative reactions causing the conversion of NO to NO_2 through reaction with atomic oxygen (R1) and ozone (R2).

Table 1. *Oxidation and reduction reaction mechanism of NO and NO_2.*

$NO + O \rightarrow NO_2$	$k = 1.4 \times 10^{-12}\ cm^3/s$	(R.1)
$NO + O_3 \rightarrow NO_2 + O_2$	$k = 1.8 \times 10^{-14}\ cm^3/s$	(R.2)
$O_2 + e \rightarrow O + O + e$	$k = 1.1 \times 10^{-12}\ cm^3/s$	(R.3)
$O_2 + O \rightarrow O_3$	$k = 1 \times 10^{-14}\ cm^3/s$	(R.4)
$NO + N \rightarrow N_2 + O$	$k = 2.1 \times 10^{-11}\ cm^3/s$	(R.5)
$N_2 + e \rightarrow N + N + e$	$k = 3 \times 10^{-16}\ cm^3/s$	(R.6)
$NO + N_2(A) \rightarrow N_2 + N + O$		(R.7)
$N_2 + e \rightarrow N_2(A) + e$	$k = 3.4 \times 10^{-11}\ cm^3/s$	(R.8)
$NO + OH \rightarrow HNO_2 + M$	$k = 2.5 \times 10^{-12} cm^3/s$	(R.9)
$NO_2 + OH \rightarrow HNO_3 + M$	$k = 4.11 \times 10^{-11}\ cm^3/s$	(R.10)
$e + H_2O \rightarrow OH + H + e$	$k = 6.8 \times 10^{-12}\ cm^3/s$	(R.11)

Oxygen atoms and ozone molecules were produced as a result of electron impact dissociation of oxygen molecules in the discharge zone (R3 & R4). The reductive reaction described in (R5) causing the conversion of NO into N_2 through the reaction between NO and atomic nitrogen N that formed as a result of electron impact dissociation of N_2 inside the discharge zone (R6). The NO reduction into N_2 achieved under the condition that nitrogen atoms exceeds oxygen atoms otherwise the oxidative reaction described in reaction (R1) will be dominant [30]. NO could also be reduced to N_2 (R7) through reaction with nitrogen molecules metastables $N_2(A)$ formed as a result of electron excitation of nitrogen molecule described in reaction (R8). NO and NO_2 in the presence of OH radicals are rapidly converted to nitrous (HNO_2) and nitric (HNO_3) acids as shown in reactions (R9 & 10) respectively. OH radicals formed as a result of water vapor electron impact dissociation described in (R11). The discharge length is anther effective factor in NOx reduction as shown in Figure 8. Increasing the discharge length cause an increase in the number of microdischarge inside the discharge zone, which enhance the chemical reactions inside the discharge zone, followed by an increase in removal efficiency. Increasing the discharge length causes an increase in the discharge volume followed by an increase in the residence time inside the discharge zone that enables more interaction between plasma species and treated gases

Consumed power is another important factor affecting the removal efficiency of NO_x. Increasing the consumed power will contribute to increase the electron density and electron temperature those have a positive contribution to electron impact dissociation and excitation of oxygen, nitrogen and water vapor molecules those form free radicals like O, N, O_3 and OH whom are contributing in NOx reduction.

3.3. Specific Energy Density

Specific energy density (SED) is defined as discharge power per unit gas volume, measured in J/L. The specific energy density for NO_x reduction can be calculated from the following formula:

$$SED\ (J/L) = \frac{input\ power\ (W)}{Flow\ rate\ (L/s)} \quad (4)$$

The concentration of NO_x as a function of the specific energy density can be seen in figure 9. It is evident from the figure that the concentration of NO_x steadily decreases with the increase of SED for all discharge lengths. This signifies that the increase in SED cause an increase in electron density and electron temperature that produce more radicals those contribute in the removal of NO_x. Also, it can be observed that, with increasing the discharge length, more SED is needed to be conducted in order to achieve more NO_x reduction. At discharge length of 120 cm maximum reduction in NO_x concentration has been achieved, on the other side a lot of SED has been consumed. So increasing the discharge length will improve the reduction in NOx concentration, but it will necessitate more energy to be added to the discharge zone.

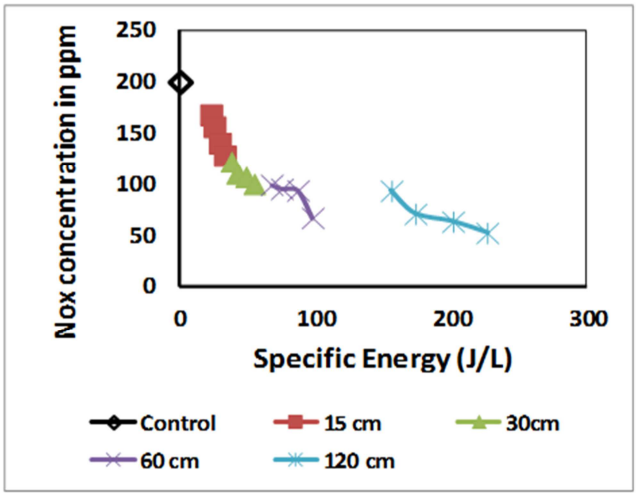

Figure 9. *The specific energy density for NOx reduction.*

3.4. Energy Cost

The standard of performance for pollution control devices is the energy required to remove a given quantity of pollutant. In the case of plasma devices removing dilute concentrations of pollutants, the performance is best described in terms of the number of eV required to remove each pollutant molecule. Energy cost is the amount of energy required to remove one molecule of NO_x from the discharge zone. It can be calculated from the following formula:

$$\text{Energy Cost (eV/molecule)} = \frac{power\ input(W)\times 6.25\times 10^{18} eV/sec}{NO_x\ molecules\ Removed} \quad (5)$$

Figure 10 shows the relation between the energy cost in eV/molecule and the removal efficiency of NO_x at different discharge length.

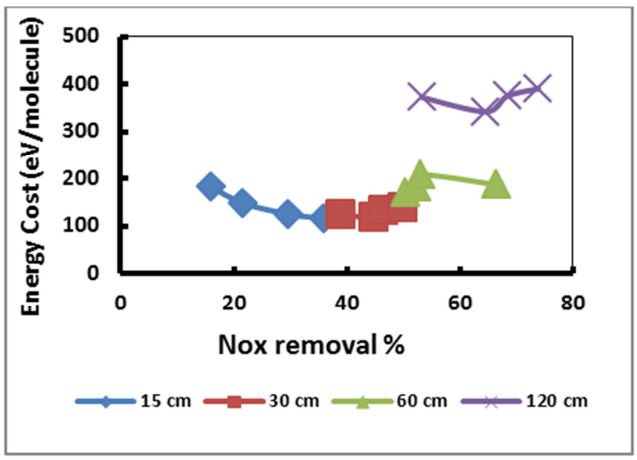

Figure 10. *Energy Cost as a function NOx removal Efficiency.*

The curve shows that high removal efficiency requires high energy cost. Removal efficiency from 50%-66% requires energy cost range from 170-187 eV/molecule at discharge length of 60 cm while removal efficiency range from 53% to 74% requires energy cost from 372 to 392 eV/molecule at discharge length 120 cm, this is because high removal efficiency needs more consumed power to enhance the removal process. A discharge length of 30 cm shows small values of energy cost that range from 123-139 eV/molecule corresponding to moderate removal efficiency that range from 39% to 50%.

4. Conclusion

This article deals with non equilibrium plasma process for removal of nitrogen oxides. An efficient coaxial dielectric barrier discharge reactor with variable discharge length was constructed for maximum removal efficiency and low energy cost. Based on the approach presented in the current work conversion efficiency was strongly dependent upon the consumed power and discharge length. It was also found that increasing the discharge length will improve the efficiency of NO_x reduction but it will necessitate more energy density and energy cost to be added to the discharge zone. Even though the efficiency improvement could be achieved by using different types of catalysts inside the plasma reactor those help in increasing NO_x reduction efficiency and reduce energy cost.

References

[1] A. Chaloukou, I. Mavroidies, I. Gavriil "Compliance with the annual NO_2 air quality standard in Athens. Required NOx levels an expected health implications". Atmospheric environment Vol. 42, 2008, pp. 454-465.

[2] WHO Review of evidence on health aspects of air pollution — REVIHAAP Project, Technical Report, World Health Organization, Regional Office for Europe, Copenhagen. 2013

[3] EEA Report No 28/2016. Air quality in Europe, European Environment Agency 2016.

[4] WHO. Health risk assessment of air pollution general principles. World Health Organization, Regional Office for Europe, Copenhagen 2016

[5] Selective Catalytic Reduction Control of NOx Emissions, SCR Committee of Institute of Clean Air Companies. 1997

[6] Netherlands Organization for Scientific Research. "Economical And Cleaner Cars With Lean-burn Catalytic Converter." ScienceDaily. 17 July 2007.

[7] Empa. "Diesel exhaust gases without any nitric oxides – is that possible." ScienceDaily. 1 October 2015.

[8] S. Müller, R. J Zahn, "Air pollution control by non-thermal plasma", Special Issue of 13th Topical Conference on Plasma Technology, Vol. 47, Issue 7, 2007, pp. 520–529.

[9] B. Haryanto Air Pollution - A Comprehensive Perspective, InTech, Chapters 2012

[10] D. Wang, T. Namihira, H. Akiyama. Pulsed discharge plasma for pollution control, Air Pollution, Vanda Villanyi (Ed.), 2010

[11] N. Takamura, D. Wang, D. Seki, T. Namihira, K. Yano, H. Saitoh, H. Akiyama,. International Journal of Plasma Environmental Science & Technology, Vol. 6, No. 1, 2012, pp. 59- 62.

[12] T. Oda. Atmospheric pressure nonthermal plasma decomposition of gaseous air contaminants and that diagnosis, ICESP X June Australia, 1A1, 2006, pp1-14.

[13] A. Fridman, Plasma Chemistry Cambridge University Press, New York 2008

[14] F. Alexander, L. A Kennedy, "Plasma Physics and Engineering", CRC press 2004.

[15] J. Park, I. Henins, H. W. Herrmann, G. S. Selwyn, J. Y. Jeong, R. F. Hicks. "An atmospheric plasma source" Applied Physics Letters Vol 76 (3) 2000, pp288-290.

[16] B. Eliasson, U. Kogelschatz "Modeling and application of silent discharge plasmas" IEEE Transaction on Plasma Science; Vol 19 (2), 1991, pp 309-323.

[17] M. O. Bratislav, B. S. Goran, M. K. Milorad "A dual-use of DBD plasma for simultaneous NOx and SO_2 removal from coal-combustion flue gas" Journal of Hazardous Materials Vol 185 (2–3), 2011, pp. 1280–1286.

[18] T. Yamamoto, B. S. Rajanikanth, M. Okubo, T. Kuroki, and M. Nishino "Performance evaluation of nonthermal plasma reactors for NO oxidation in diesel engine exhaust gas treatment" IEEE Transactions on Industry applications, vol. 39, 2003, pp. 1608-1613.

[19] B. S Rajanikanth and D. Sinha. Achieving better NOx removal in discharge plasma reactor by field enhancement," Plasma Science and Technology, vol. 10, 2008, pp. 198-202.

[20] T. Kuwahara, T. Kuroki, H. Nakaguchi, M. Okubo Continuous reduction of cyclic adsorbed and desorbed NO_x in diesel emission using nonthermal plasma Journal of hazardous materials 308 2016

[21] M. Okubo, H. Yamada, K. Yoshida, T. Kuroki "Simultaneous Reduction of Diesel Particulate and NOx Using Catalysis Combined Nonthermal Plasma Reactor" Proc. Electrostatics Joint Conference 1-13, 2016

[22] M. Okubo, T. Kuroki, K. Yoshida, and T. Yamamoto, "Single-stage Simultaneous Reduction of Diesel Particulate and NOx Using Oxygen-Lean Nonthermal Plasma Application" IEEE Trans. Ind. Appl., vol. 46, no. 6, 2010, pp. 2143–2150.

[23] M. Okubo, N. Arita, T. Kuroki, K. Yoshida, and T. Yamamoto, "Total diesel emission control technology using ozone injection and plasma desorption," Plasma Chem. Plasma Process., vol. 28 (2), 2008, pp. 173–187.

[24] T. C. Manley "The Electric Characteristics of the Ozonator Discharge". Trans. Electrochem. Soc. 84 (1), 1943, pp. 83-96.

[25] U. Kogelschatz, "Dielectric-barrier discharges: Their history, discharge physics and industrial applications" IEEE Trans. Plasma Sci., vol. 30 (4), 2002, pp 1400–1408.

[26] N. Naud´e, J-P. Cambronne, N. Gherardi and F. Massines "Electrical model and analysis of the transition from an atmospheric pressure Townsend discharge to a filamentary Discharge" J. Phys. D: Appl. Phys. Vol. 38, 2005, pp. 530–538.

[27] U. Kogelschatz, B. Eliasson, W. Egli. « Dielectric-Barrier Discharges Principle and Applications ». Journal de Physique IV Colloque, Vol. 7 (C4), 1997, pp. 47-66.

[28] U. Kogelschatz, B. Eliasson and W. Egli "From ozone generators to television screens: history and future potential of dielectric-barrier discharges" Pure Appl. Chem., Vol. 71 (10), 1999, pp. 1819-1828.

[29] N. Manivannan, W. Balachandran, R. Beleca, and M. Abbod "Non-Thermal Plasma Technology for the Abatement of NOx and SOx from the Exhaust of Marine Diesel Engine" Journal of Clean Energy Technologies, Vol. 2 (3), 2014

[30] M. Penetrante, R. M Brusasco, B. T Merritt and G. E. Vogtlin "Environmental applications of low-temperature" plasmas Pure Appl. Chem., Vol. 71 (10), 1999, pp 1829-1835.